Mon. Not. R. Astron. Soc. (1992) **259**, 465–473

Evolution of a magnetic flux tube in two-dimensional penetrative convection

R. L. Jennings,[1] A. Brandenburg,[2] Å. Nordlund[3] and R. F. Stein[4]
[1] *DAMTP, Silver Street, Cambridge CB3 9EW*
[2] *Nordita, Blegdamsvej 17, DK-2100 Copenhagen Ø, Denmark*
[3] *Copenhagen University Observatory, DK-1350 Copenhagen K, Denmark*
[4] *Department of Physics and Astronomy, Michigan State University, East Lansing, MI 48824, USA*

Accepted 1992 May 22. Received 1992 May 22; in original form 1992 March 9

ABSTRACT

Highly supercritical compressible convection is simulated in a two-dimensional domain in which the upper half is unstable to convection while the lower half is stably stratified. This configuration is an idealization of the layers near the base of the solar convection zone. Once the turbulent flow is well developed, a toroidal magnetic field $\boldsymbol{B}_{\rm tor}$ is introduced to the stable layer. The field's evolution is governed by an advection–diffusion-type equation, and the Lorentz force does not significantly affect the flow. After many turnover times the field is stratified such that $|\boldsymbol{B}_{\rm tor}|/\rho \approx$ constant in the convective layer, where ρ is density, while in the stable layer this ratio decreases linearly with depth. Consequently most of the magnetic flux is *stored* in the overshoot layer. The inclusion of rotation leads to travelling waves which transport magnetic flux latitudinally in a manner reminiscent of the migrations seen during the solar cycle.

Key words: convection – MHD – Sun: interior – Sun: magnetic fields – sunspots.

1 INTRODUCTION

A widely held view (see, for example, Weiss 1989) is that solar magnetic fields are generated by an $\alpha\omega$-dynamo near the base of the convection zone (CZ). In this picture, field accumulates deep in the CZ until there is an instability driven by magnetic buoyancy causing a toroidal flux tube to rise through the CZ. This tube eventually bursts through the photosphere at two points, producing a pair of sunspots. The fact that spots appear at only one or two longitudes suggests that the instability is a kink mode, as in Moreno-Insertis (1986). Flux tubes rising through the CZ have been modelled by several authors (Parker 1979; Moreno-Insertis 1983, 1986; Choudhuri & Gilman 1987; Petrovay 1991), resulting in estimates for the rise time to the surface of a month. Convection was, however, omitted in these models, and the tube is assumed to rise through a stratified gas due to its buoyancy. Furthermore, if rotation is included, the tubes are deflected so far poleward that they reach the solar surface at latitudes much higher than the main sunspot belts (Choudhuri & Gilman 1987). This motivated Choudhuri & D'Silva (1990) to include turbulent drag as well as rotation, but the tubes were still deflected poleward.

In this work we directly simulate the evolution of a flux tube through a layer of highly supercritical compressible convection. Moreover, we include rotation and a stably stratified layer at the base of the CZ which models the Sun's radiative interior. This stable layer plays an important rôle in the tube's evolution. No attempt is made to resolve the fine structure just beneath the solar surface, and we impose idealized boundary conditions at the top of the domain. Indeed, we formulate as simple a model as possible by restricting attention to a small Cartesian chunk of the Sun in which the flow is two-dimensional (2D) and there is no dynamo action. It transpires that a single component of magnetic field $B_y\hat{\boldsymbol{y}}$ is sufficient to model a toroidal flux tube in this set-up. In the absence of magnetic fields and rotation the initial polytropic equilibrium and governing equations are the same as in Hurlburt, Toomre & Massaguer (1986). Rather than reproduce such details here the reader is referred to that paper, where there is a full account of 2D compressible penetrative convection. Recently, Nordlund et al. (1992) extended the work of Hurlburt et al. into three dimensions in their direct simulation of a dynamo.

The numerical experiment begins once the convection is well developed, at which point the magnetic tube is inserted

in the stable layer and *let go*. After this we follow the tube's evolution. In the next section the model is described. Then in Sections 3 and 4 the evolution is described in the absence and presence of rotation respectively. A brief discussion follows in Section 5.

2 THE MODEL

We consider a small piece of the sphere located 30° south of the equator. Neglecting curvature we replace spherical coordinates (r, θ, ϕ) by Cartesians (z, x, y) respectively, with gravity $\boldsymbol{g}=g\hat{\boldsymbol{z}}$, where x points north, y east, and z downwards. We adopt the f-plane approximation of oceanography (see, for example, Gill 1982), thus the rotation vector $\boldsymbol{\Omega}=\frac{1}{2}\Omega(\sqrt{3}\hat{\boldsymbol{x}}+\hat{\boldsymbol{z}})$ is independent of x.

All quantities are assumed to be independent of y (analogous to being axisymmetric). The planar domain S is a square of side $2d$, and is only convectively unstable in the upper half: $0\le z\le d$, where $z=0$ is the upper boundary. Perturbing the equilibrium therefore leads to penetrative convection, as well as gravity waves in the lower layer.

Periodic boundary conditions are used at $x=0$ and $x=2d$. The top surface $(z=0)$ is isothermal, while a constant heat flux is imposed at the bottom. Both surfaces are stress-free, impenetrable perfect conductors. These conditions isolate the domain.

We solve the equations of rotating compressible magneto-convection using the perfect gas law, $p=(\gamma-1)\rho e$, where p, ρ and e are pressure, density and internal energy respectively, and $\gamma\equiv c_p/c_v=5/3$ is the ratio of specific heats. As the fluid is compressible, there is the characteristic up–down asymmetry whereby downdrafts are stronger and narrower than updrafts.

In accordance with the idea that the solar dynamo is of $\alpha\omega$-type, we assume that the toroidal field component B_y is much larger than the poloidal components. Hence we consider $\boldsymbol{B}=(0, B_y, 0)$, which is only introduced once the convection is established. Clearly $\nabla\cdot\boldsymbol{B}=0$, and an application of the divergence theorem shows that the integral $\int_S B_y \mathrm{d}x\,\mathrm{d}z$ is time-independent. We used this condition as a numerical check and obtained satisfactory results.

To model a flux tube which is initially in the stable layer, we assume $B_y(x, z)$ has a Gaussian distribution centred at $x=1, z=1.25$:

$$B_y=B_0\exp\{-100[(x-1)^2+(z-1.25)^2]\}.$$

Thus the magnetic field and its derivatives are continuous everywhere. Since $(\boldsymbol{B}\cdot\nabla)\,\boldsymbol{u}=0$, the field components B_x and

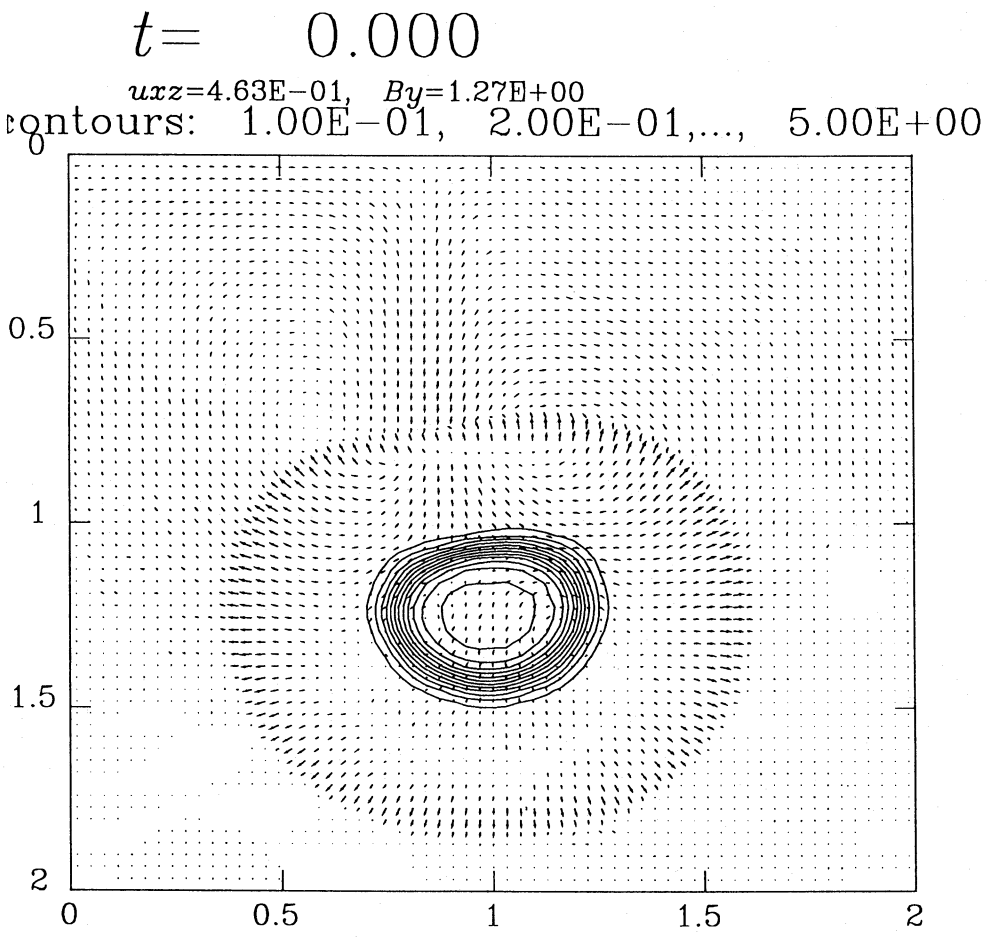

Figure 1. Sound waves signal the introduction of a strong toroidal magnetic field: $Q=10^8$. Here, and in similar plots, B_y is represented using contours and arrows are velocity vectors. In this plot the sound waves have a larger amplitude than the convection, and the code soon crashes. This does not happen with $Q=10^6$ where the shock to the system is smaller. Note that the upward propagating wave is slower due to the variation of sound speed with depth.

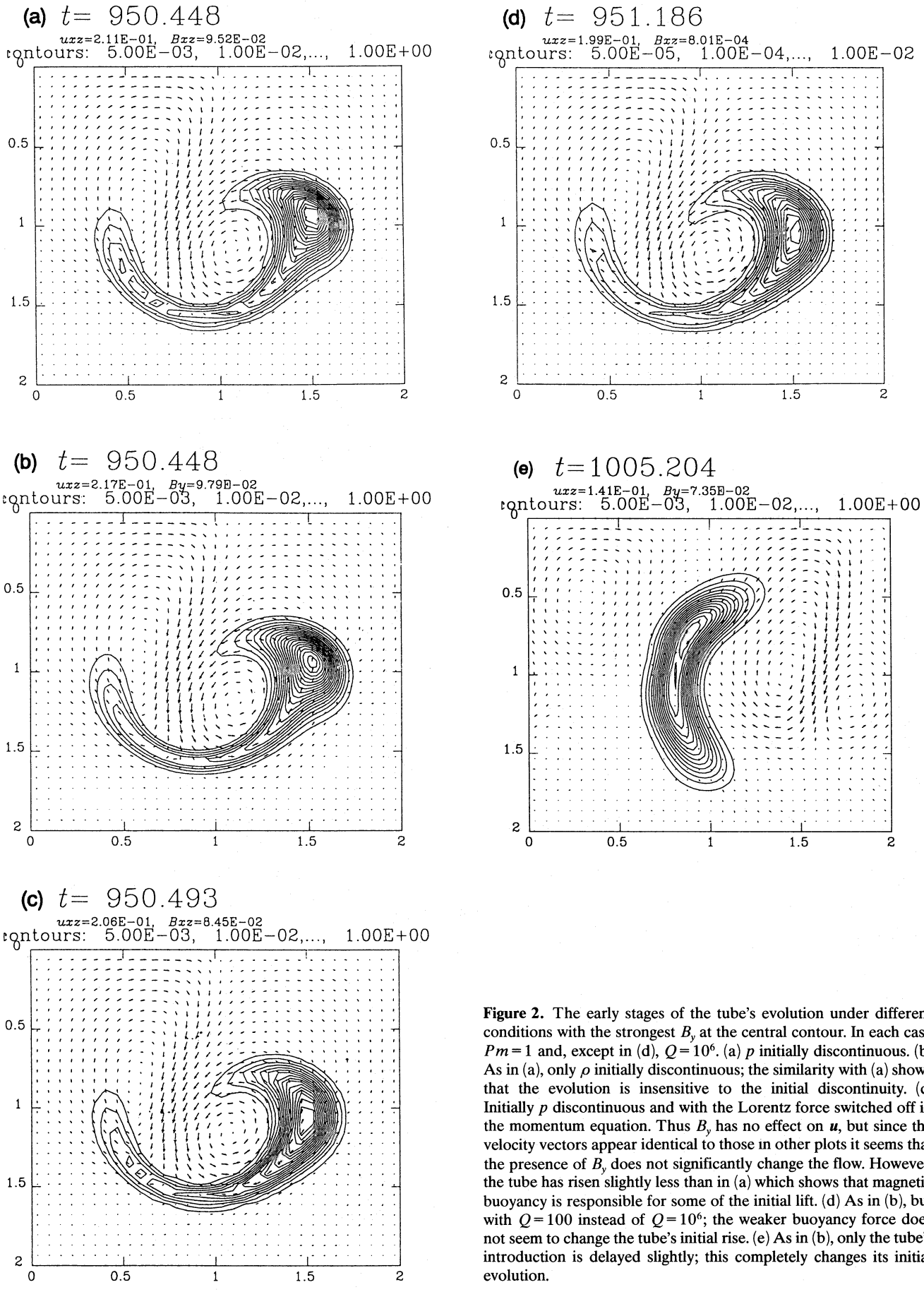

Figure 2. The early stages of the tube's evolution under different conditions with the strongest B_y at the central contour. In each case $Pm = 1$ and, except in (d), $Q = 10^6$. (a) p initially discontinuous. (b) As in (a), only ρ initially discontinuous; the similarity with (a) shows that the evolution is insensitive to the initial discontinuity. (c) Initially p discontinuous and with the Lorentz force switched off in the momentum equation. Thus B_y has no effect on $\boldsymbol{u}$, but since the velocity vectors appear identical to those in other plots it seems that the presence of B_y does not significantly change the flow. However, the tube has risen slightly less than in (a) which shows that magnetic buoyancy is responsible for some of the initial lift. (d) As in (b), but with $Q = 100$ instead of $Q = 10^6$; the weaker buoyancy force does not seem to change the tube's initial rise. (e) As in (b), only the tube's introduction is delayed slightly; this completely changes its initial evolution.

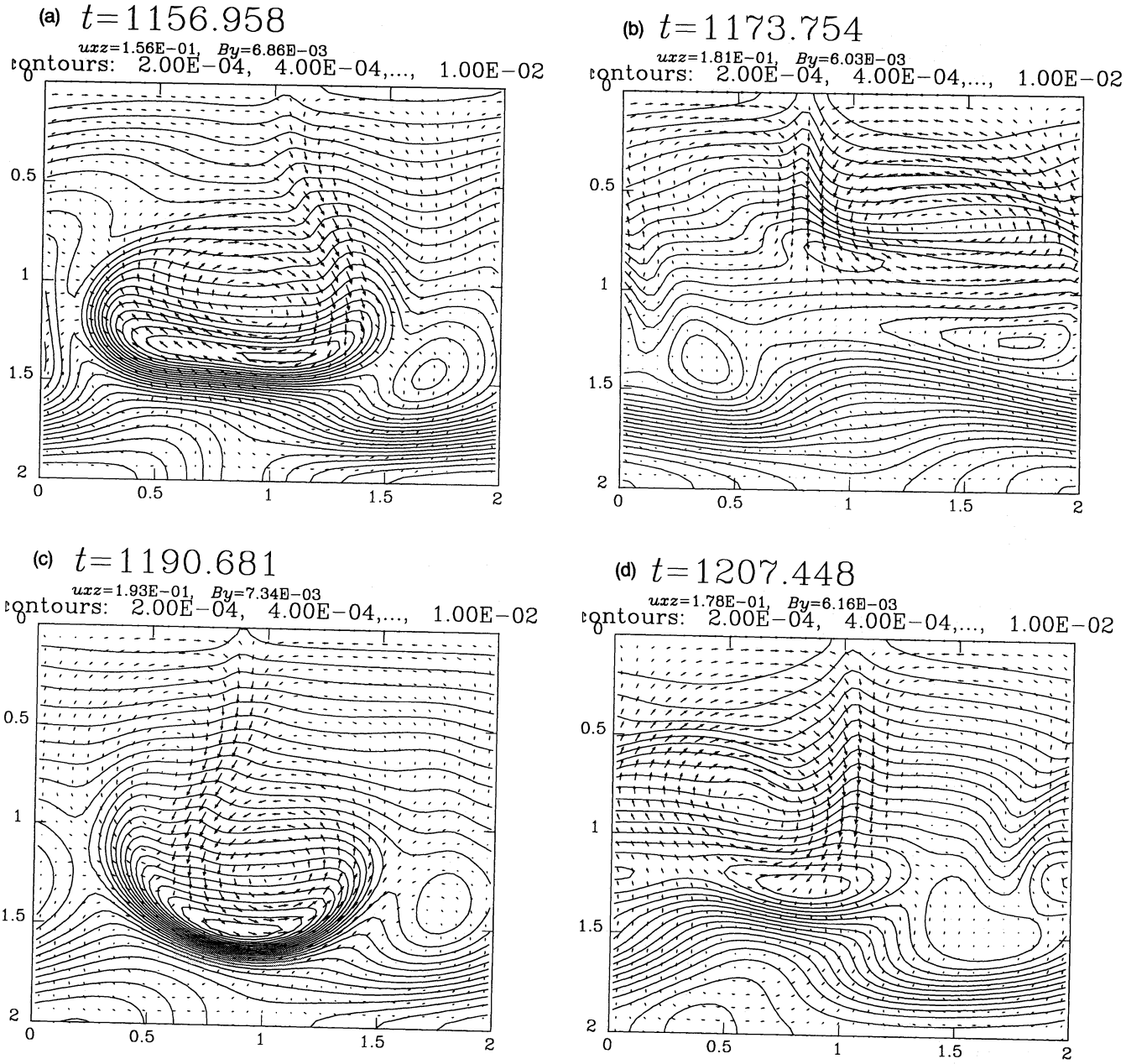

Figure 3. Long after the tube's introduction the stratified field is intermittently squeezed by descending fluid in downdrafts. Between such times it can relax to a more uniform stratification. These plots with $Pm=1$ and $Q=10^6$ are typical, and (a)–(d) show successive snapshots at intervals of 17 time units. The maxima of B_y occur in the eye-like contours around $z=1.4$.

B_z remain zero for all time, leaving only the y-component of the magnetic induction equation non-trivial. Using the continuity condition $\mathrm{D}\rho/\mathrm{D}t+\rho\nabla\cdot\boldsymbol{u}=0$, where velocity $\boldsymbol{u}=(u, v, w)$ and $\mathrm{D}/\mathrm{D}t=\partial_t+(\boldsymbol{u}\cdot\nabla)$, the induction equation can be expressed as

$$\rho\mathrm{D}(B_y/\rho)/\mathrm{D}t=\eta\nabla^2 B_y, \tag{1}$$

with magnetic diffusivity η. Thus the evolution of B_y is governed by advection and diffusion. In addition, the Lorentz force modifies the momentum balance and electric currents $\boldsymbol{J}$ dissipate heat. The momentum and energy equations become

$$\rho\left(\frac{\mathrm{D}\boldsymbol{u}}{\mathrm{D}t}+2\Omega\times\boldsymbol{u}\right)=-\nabla\left(p+\frac{B_y^2}{2\mu_0}\right)+\rho\boldsymbol{g}+\nabla\cdot(2\nu\rho\boldsymbol{S}), \tag{2}$$

and

$$\rho\frac{\mathrm{D}e}{\mathrm{D}t}=-p\nabla\cdot\boldsymbol{u}+\nabla[\mathscr{K}(z)\nabla e]+2\nu\rho\boldsymbol{S}^2+\mu_0\eta\boldsymbol{J}^2, \tag{3}$$

respectively, where $\mathscr{K}(z)$ is the thermal diffusivity, and constants μ_0 and ν are magnetic permeability and kinematic

viscosity respectively. Also, $\boldsymbol{S}$ represents the symmetric tensor $S_{ij}=\frac{1}{2}(\partial_j u_i+\partial_i u_j-\frac{2}{3}\delta_{ij}\partial_k u_k)$ with $\nabla\cdot(\nu\rho\boldsymbol{S})$ meaning $\partial_i(\nu\rho\boldsymbol{S}_{ij})$ etc. Note that B_y produces a magnetic pressure in the momentum equation, but due to its lack of curvature it does not impart any tension forces.

2.1 Dimensionless parameters

We rescale by setting $d=c_p=\overline{\rho}=\mu_0=g=1$, where $\overline{\rho}$ is the averaged density. Thus time is measured in units of $(d/g)^{1/2}$, which is related to the free-fall time of the CZ. This introduces dimensionless parameters such as the Taylor number $Ta=4\Omega^2d^4/\nu^2$ and the Prandtl number $Pr=\nu/\overline{\chi}$, where $\overline{\chi}=\mathscr{K}(z_m)/\overline{\rho}$ with $z_m=1/2$ the mid-depth of the convectively unstable layer. Additionally, the initial stratification is parametrized by $\xi_0=e(z=0)/dgm_{\rm ad}$, where $m_{\rm ad}=3/2$ is the polytropic index of an adiabatically stratified layer. Decreasing ξ_0 increases the initial density contrast between the top and bottom of the box. A Rayleigh number Ra is defined in terms of the initial entropy gradient at z_m:

$$Ra=(gd^4/\nu\overline{\chi})(\mathrm{d}s/\mathrm{d}z)\,{}^{z=z_m}_{t=0}\,.$$

Finally, the magnetic Prandtl number $Pm=\nu/\eta$, and the initial strength of the magnetic tube is measured by the Chandrasekhar number $Q=B_0^2d^2/\mu_0\overline{\rho}\nu\eta$.

In all that follows $Ra=10^5$ ($400\times$ supercritical when $Ta=0$, but only about $50\times$ supercritical with $Ta=10^4$), $Pr=0.2$ and $\xi_0=0.5$ (density contrast ≈ 4), which makes $\nu=5.16\times10^{-4}$. Both Pm and Q are varied, but typically $Q=10^6$ and $Pm=1$. With Pm of order unity η is small, and magnetic flux is virtually frozen into the plasma, as is believed to be the case in the Sun. Using these parameters the Reynolds number $Re=U_{\rm max}\,d/\nu=O(100)$, and since the Sun's Rossby number is $O(1)$, we take $Ta=10^4$ in cases with rotation. Without rotation $Ta=0$, and there is no azimuthal velocity v. For $Q=10^6$ the ratio of magnetic to kinetic energy is initially around 10^{-3}.

Numerical solutions were obtained using a modified version of the code described in Brandenburg et al. (1990), where spatial derivatives are obtained from cubic spline approximations. Solutions are then time-stepped using a second-order Adams–Bashforth scheme. Here we take a uniform grid of 63^2 points, which provides sufficient resolution for the parameters considered.

3 RESULTS WITH NO ROTATION

When the tube is first introduced the total pressure (gas plus magnetic) is instantaneously increased. However, it does not have to be the pressure which is discontinuous initially, and the tube can be added such that any one quantity such as p,

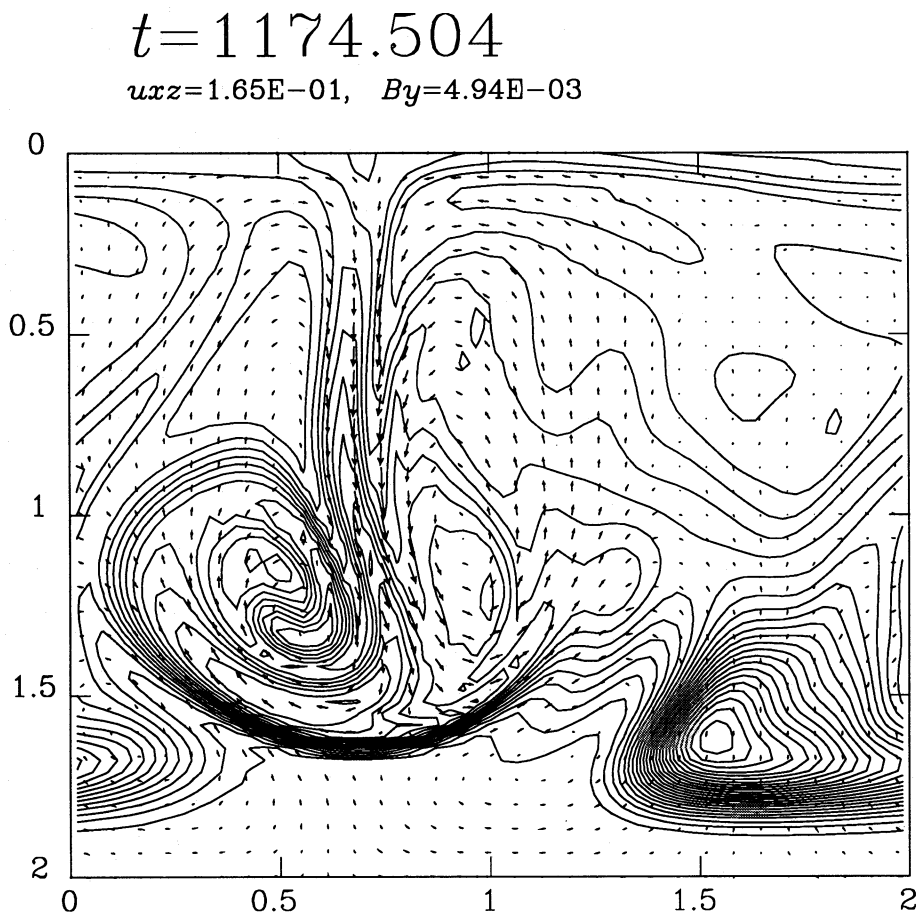

Figure 4. Increasing Pm leads to more structure in B_y. This snapshot, with $Pm=10$, shows the field being wound up after it has been transported to the base of the CZ by a strong downdraft.

ρ, e or s is discontinuous. It turns out, however, that the tube's rise is insensitive to the initial conditions; see Figs 1 and 2. This is because sound waves rapidly smooth out any pressure discontinuities and, since the Prandtl number is small, thermal diffusion is effective to make the tubes behave almost isothermally.

When the tube is added it exerts a large magnetic pressure force outwards in all directions from its centre. There is also considerable diffusion associated with the sharp peak in its distribution. Thus the field diffuses outwards in all directions. Yet the expansion of field is primarily upwards into the lighter fluid, and it soon enters the CZ. There it is strongly advected and any memory of the initial conditions is soon lost. Comparison of the different plots in Fig. 2 shows that magnetic buoyancy is not important during the tube's initial rise, since the initial rise is independent of magnetic field strength. The boundary conditions at the top of the box preclude the tube escaping and so the field continues to be advected. After a few turnover times the magnetic field fills the whole domain and settles to a statistically steady state in which it is stratified with depth. Even though some toroidal flux escapes the Sun's CZ, it is argued by Parker (1984) that it is primarily confined to the CZ. If so, the perfectly conducting upper boundary is appropriate, and the results presented here may well be relevant to the Sun.

At times when the downdrafts are strong the field in the overshoot layer is squeezed by descending fluid. As the downdraft weakens, the field relaxes to a more uniform stratification but at all times there are localized tube-like concentrations of field stored in the stable layer; see Fig. 3. This squeeze–relax cycle repeats almost periodically. Increasing Pm leads to finer structure in B_y (see Fig. 4), but the field's evolution is qualitatively unaffected. Referring back to equation (1) it is not surprising to find that the magnetic field is stratified such that $\langle B_y/\rho\rangle \approx$ constant, where the angled brackets denote horizontal averaging; see Fig. 5. Varying Q does not change this scenario, implying that the magnetic pressure in the momentum equation is relatively unimportant for $Q \leq 10^6$. Fig. 6 shows time series of the Nusselt number Nu (usual definition with $Nu > 1$ once convection begins), and the plasma beta: $\beta = (p_{\rm gas}/p_{\rm mag})$, where the instantaneous β is evaluated at the point in S with the largest $p_{\rm mag}$. At the bottom of the solar CZ, $p = 3 \times 10^{14}$ g cm^{-1} s^{-2}, i.e. $\beta = 10 \ldots 10^5$ (cf. Fig. 6b) would correspond to $B_{\rm max} = 2$ MG … 200 G.

4 RESULTS WITH ROTATION

With rotation the convection is much less supercritical and therefore less vigorous. The Coriolis force transfers

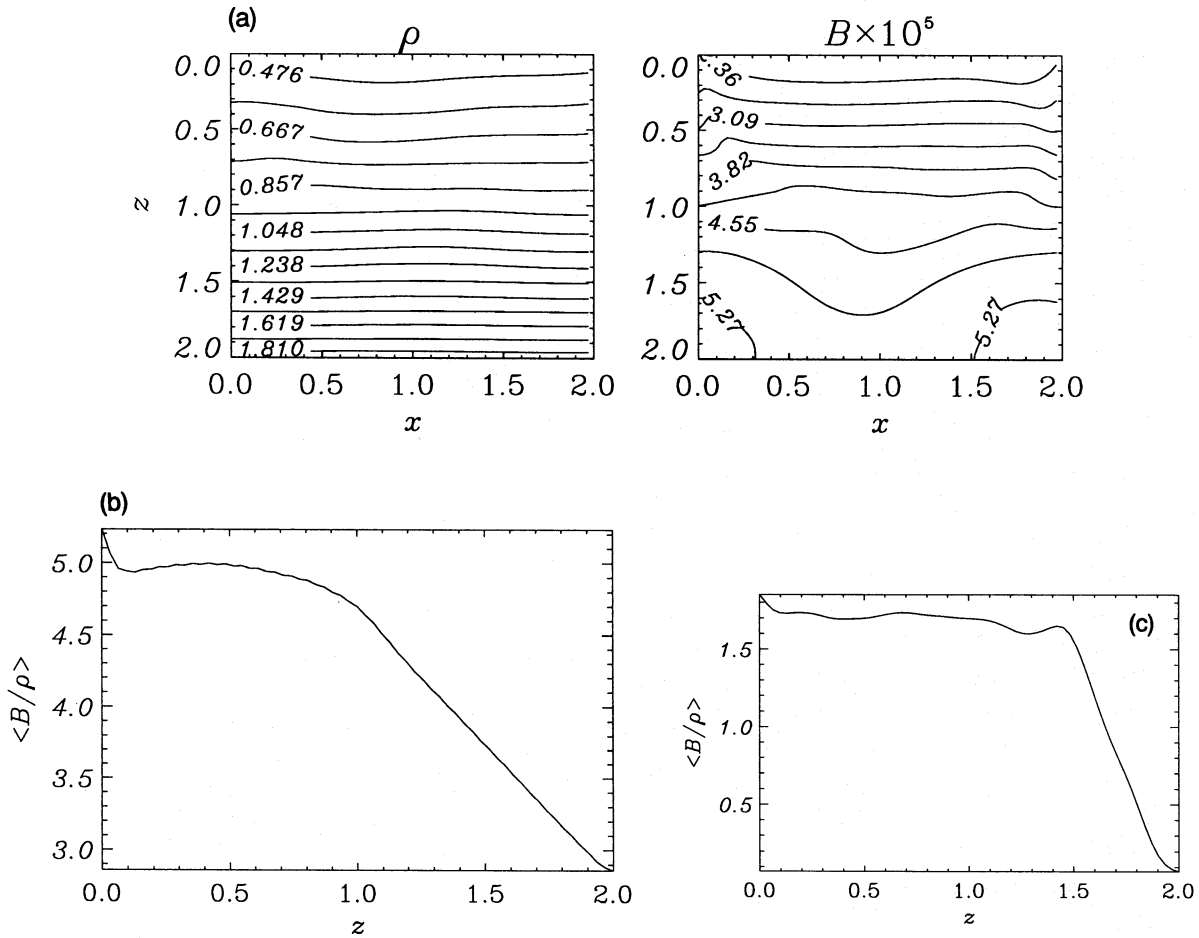

Figure 5. Contours of (a) ρ and B_y for the run in Fig. 3 only at a much later time. (b) $\langle B_y/\rho\rangle$, which is almost constant in the CZ, but decreases linearly in the stable layer. (c) As in (b), only with $Pm = 10$, in which case $\langle B_y/\rho\rangle$ is approximately constant until $z = 1.5$.

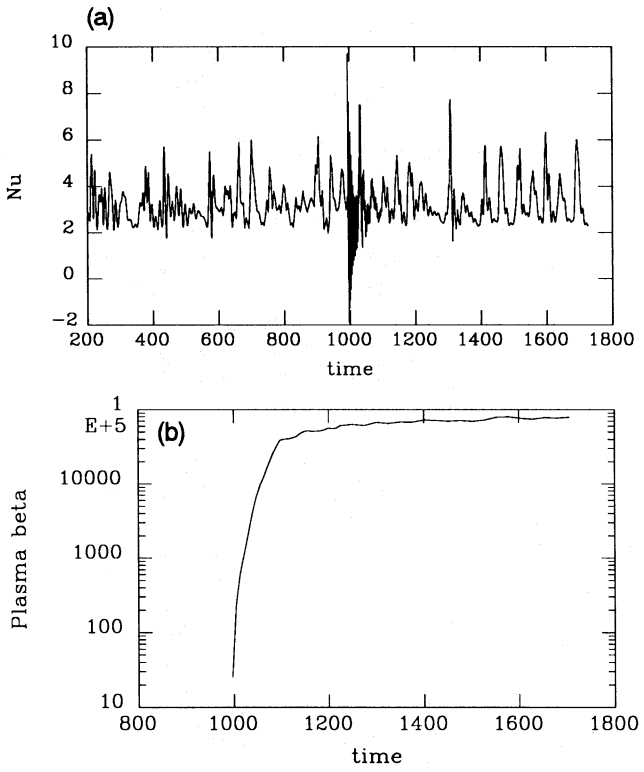

Figure 6. (a) $Nu(t)$; the tube is introduced just before $t=1000$ and the resulting discontinuity makes Nu oscillate wildly at high frequency (sound waves), although these oscillations soon decay. The aperiodic oscillations with longer periods are associated with gravity waves, and arguably they are more regular for $t>1400$ than at earlier times when there was no magnetic field. This suggests the field has a stabilizing influence upon the convection. (b) $\beta(t)$. Since p_{gas} is almost independent of time the increase in $\beta(t)$ is associated with the decline in the maximum of p_{mag} as B_y is distributed more evenly throughout S.

momentum into the y-direction so that $Dv/Dt \neq 0$ and there is an azimuthal flow. Solutions also drift in x, that is, they are travelling waves. Contours of $v(x, z)$ at different times using $Q=10^6$ (Fig. 7) show the wave crossing S from right to left (equatorward).

As before, the magnetic field rises. It also drifts in the direction of the wave (Fig. 8a), only more slowly. After many turnover times B_y is stratified with depth (Fig. 8b), and $\langle B_y/\rho \rangle$ in Fig. 8(c) has a similar profile to that in Fig. 5(b). Graphs of $Nu(t)$ and $\beta(t)$ are in Fig. 9.

5 DISCUSSION

The most important outcome from this simulation is the finding that long after the tube's introduction the magnetic field becomes stratified such that $\langle B_y/\rho \rangle \approx$ constant in the CZ. This final state is independent of the initial conditions and may well reflect conditions inside the solar CZ. Beyond a certain depth, however, this stratification no longer holds and $\langle B_y/\rho \rangle$ declines to zero. Nevertheless, the flux in the overshoot layer exceeds that in the CZ by about 30 per cent and, altogether, more than 80 per cent of the flux is concentrated within one density scaleheight of the base of the CZ.

According to Stenflo (1991), photospheric magnetic flux at active longitudes is replenished by new flux from deep inside the CZ in a time-scale considerably shorter than the Sun's rotation period. This suggests that advection may be more important than buoyancy in bringing up new flux to the solar surface. We expect that the advection effects would be even more pronounced if the tube were released in the unstable region. In our experiment, the advection of B_y dominates buoyancy and the initially circular tube rapidly deforms. Yet the absence of poloidal field in this model may be relevant, since Cattaneo, Chiueh & Hughes (1990) found that the presence of a small poloidal field greatly increases

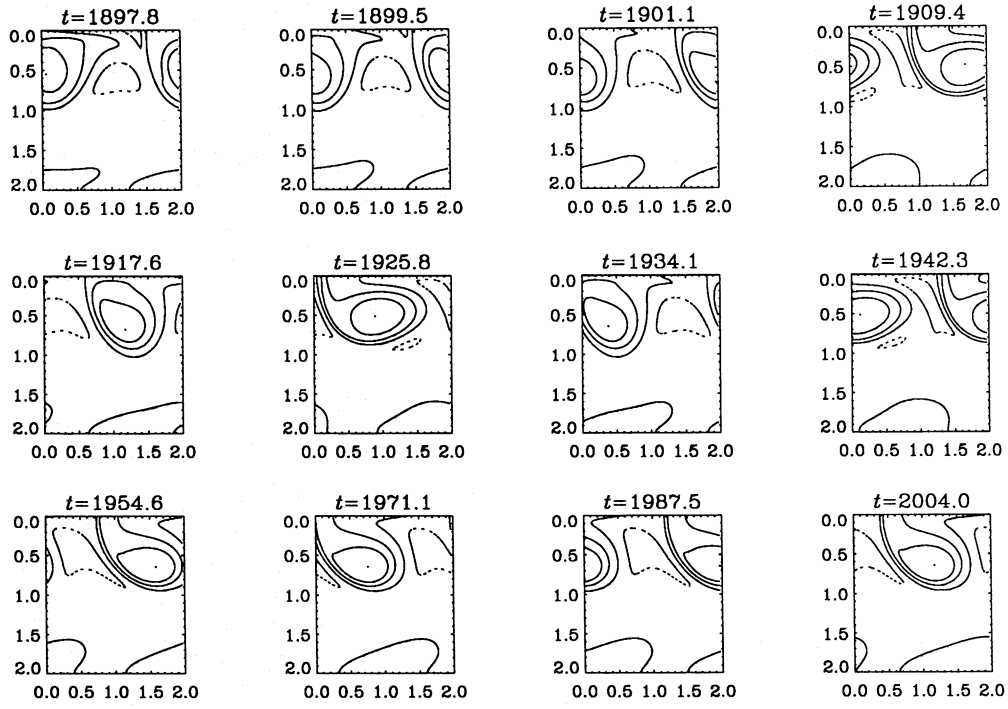

Figure 7. Contours of v (broken if $v<0$) traverse the box from right to left (equatorward) in about 40 time units.

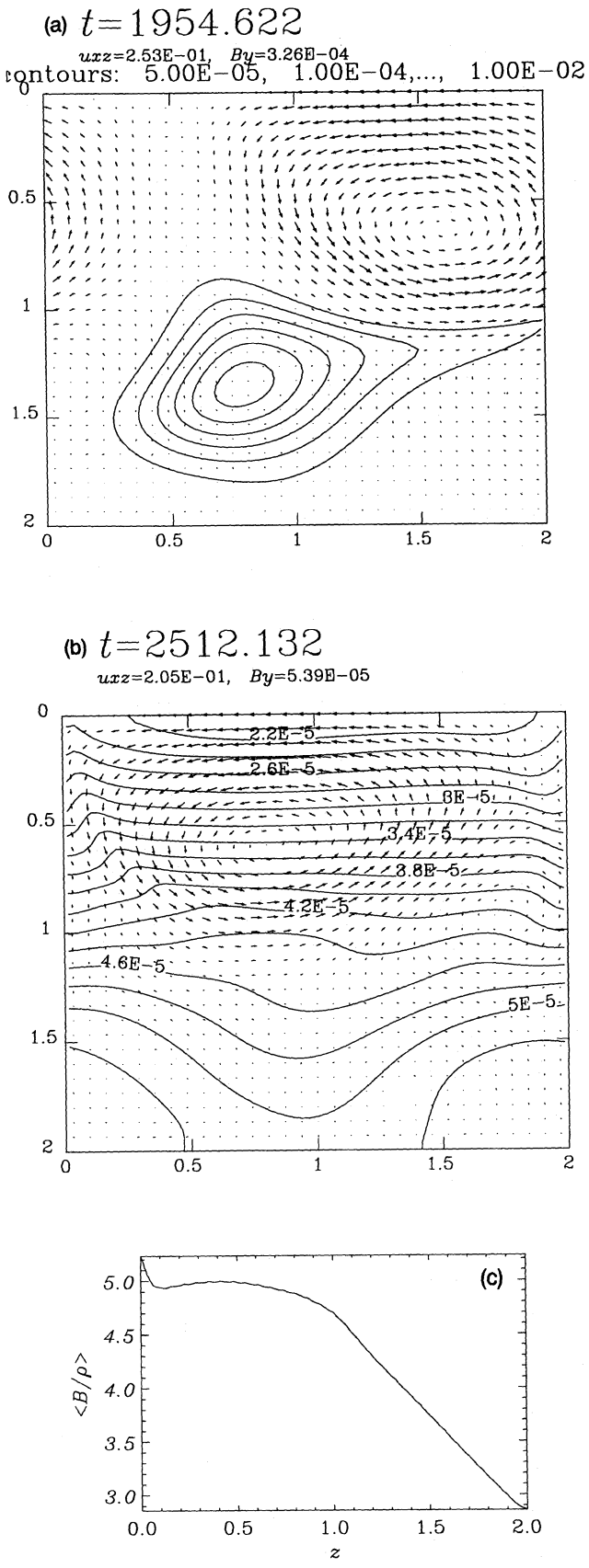

Figure 8. (a) Here $Pm = 1$ and $Q = 100$. Contours of B_y are carried along with the travelling wave, only the field is slower. (b) The field ultimately becomes stratified as before. (c) The profile $\langle B_y/\rho \rangle$, which is similar to that in Fig. 5(b).

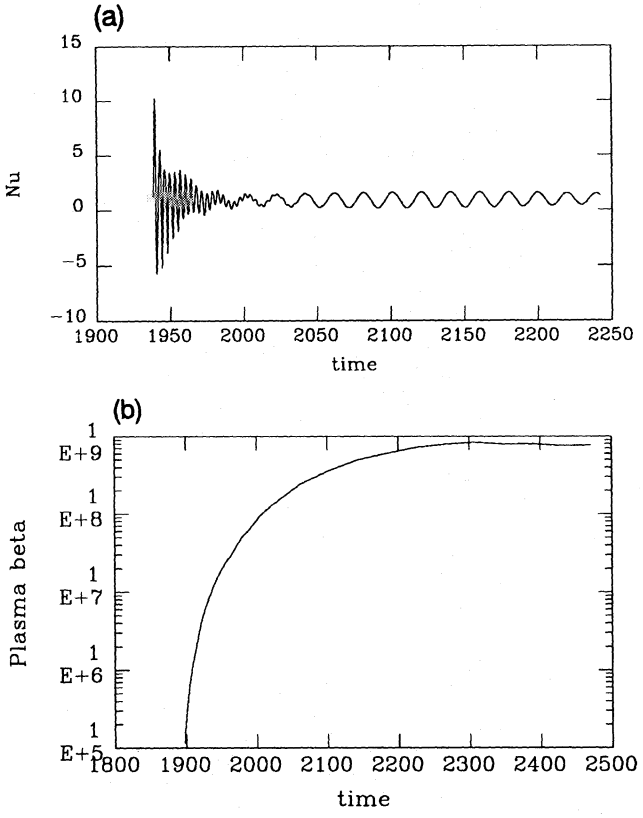

Figure 9. As Fig. 6, only with rotation and for the run described in Fig. 8. Despite appearing so, close inspection reveals that $Nu(t)$ is not strictly periodic once the transients have decayed.

the coherence of a rising toroidal flux tube. However, unlike here, the magnetic tube they considered was not entering a region of developed convection. To study these issues further it would be useful to simulate the rise of a non-axisymmetric magnetic tube through convection in spherical geometry. Perhaps then the tube would be constrained and not advected so strongly. Furthermore, a three-dimensional simulation would enable us to study the development of kink mode instabilities, which are believed to be responsible for the formation of bipolar regions (e.g. Parker 1979). The results of three-dimensional dynamo simulations by Nordlund et al. (1992) suggest that, for the model parameters used, the effects of such instabilities are weak compared with advection.

The travelling waves found when rotation is included may be an artefact of using periodic side conditions, and it is less likely that waves would occur in a spherical shell. Nevertheless such latitudinal waves are interesting since they can drag magnetic fields with them, and hence offer an alternative explanation to dynamo waves for the equatorward migrations of sunspots during the solar cycle. Again there is a need for better models to test this idea.

ACKNOWLEDGMENTS

This work was done during a visit by RLJ to Helsinki Observatory, kindly arranged by Ilkka Tuominen. All the computing was done using the Cray-XMP/432 of the Centre for Scientific Computing, Espoo, Finland. RLJ is also grateful to SERC for financial support. RFS was supported in part

by NASA grant NAGW-1695, while ÅN acknowledges support from the Danish Natural Science Research Council and the Danish Space Board.

REFERENCES

Brandenburg A., Nordlund Å., Pulkkinen P., Stein R. F., Tuominen I., 1990, A&A, 232, 277
Cattaneo F., Chiueh T., Hughes D. W., 1990, J. Fluid Mech., 219, 1
Choudhuri A. R., Gilman P. A., 1987, ApJ, 316, 788
Choudhuri A. R., D'Silva S., 1990, A&A, 239, 326
Gill A. E., 1982, Atmosphere–Ocean Dynamics. Int. Geophys. Series Vol. 30, Academic Press, Orlando
Hurlburt N. E., Toomre J., Massaguer J. M., 1986, ApJ, 311, 563
Moreno-Insertis F., 1983, A&A, 122, 241
Moreno-Insertis F., 1986, A&A, 166, 291
Nordlund Å., Brandenburg A., Jennings R. L., Rieutord M., Ruokolainen J., Stein R. F., Tuominen I., 1992, ApJ, 392, 647
Parker E. N., 1979, Cosmical Magnetic Fields. Clarendon Press, Oxford
Parker E. N., 1984, ApJ, 281, 839
Petrovay K., 1991, Solar Phys., 134, 407
Stenflo J., 1991, in Tuominen I., Moss D., Rüdiger G., eds, The Sun and Cool Stars: activity, magnetism, dynamos. Springer-Verlag, Berlin, p. 193
Weiss N. O., 1989, in Belvedere G., ed., Accretion Discs and Magnetic Fields in Astrophysics. Kluwer, Dordrecht, p. 11